



Research article

Antioxidant, α -glucosidase, antimicrobial activities chemical composition and *in silico* analysis of *eucalyptus camaldulensis* dehn

Abdulrahaman Mahmoud Dogara¹, Ateeq Ahmed Al-Zahrani^{2,*}, Sarwan W. Bradosty³, Saber W. Hamad^{4,5}, Shorsh Hussein Bapir⁶ and Talar K. Anwar⁷

¹ Biology Education Department, Tishk International University, Erbil, Iraq

² Chemistry Department, University College at Al-Qunfudhah, Umm Al-Qura University, Saudi Arabia

³ Department of Medical Laboratory Science, College of Science, Cihan University-Erbil, Kurdistan Region, Iraq

⁴ Department of Field Crops and Medicinal Plants, College of Agricultural Engineering Sciences, Salahaddin University-Erbil, Erbil, Kurdistan Region, Iraq

⁵ Department of Medical Laboratory Science, College of Science, Knowledge University, Kirkuk Road, 44001 Erbil, Iraq

⁶ Department of Horticulture, College of Agricultural Engineering Sciences, University of Raparin, Rania, Kurdistan Region, Iraq

⁷ Department of Plant Protection, College of Agricultural Engineering Sciences, Salahaddin University-Erbil, Erbil, Kurdistan Region, Iraq

* **Correspondence:** Email: aaalzahrani@uqu.edu.sa.

Abstract: Throughout history, medicinal plants have been the primary source for preventing and treating infectious diseases and other health issues. The flowering plant *Eucalyptus camaldulensis*, also called river red gum, is a member of the Myrtaceae family and has numerous traditional uses. The objectives of the present study were to identify the essential oil components of *Eucalyptus camaldulensis* using Gas Chromatography Mass Spectrometry (GCMS), and to determine the antioxidant, antidiabetic, and antibacterial activities of ethanol, aqueous, and essential oil extracts from *E. camaldulensis* leaves. Additionally, the essential oil constituents that were identified underwent an *in silico* analysis. The efficacy of various extracts in combat pathogens and free radicals was assessed through the utilization of the 1,1-Diphenyl-2-Picryl Hydrazyl (DPPH), ferric reducing antioxidant

power (FRAP), α -glucosidase inhibition, and disk diffusion methods. In terms of radical scavenging, reducing power, and α -glucosidase inhibitory activity, the essential oil showed strong antioxidant activity at 84.01 %, 20.1 mmol/g, and 78.2 %, respectively. The essential oil showed a potent antimicrobial action against *Staphylococcus aureus* and *Pseudomonas aeruginosa*, with 12 and 14 mm inhibitions, respectively, which were higher than ampicillin's 9 and 6 mm inhibitions, respectively. The GCMS analysis showed that the following chemicals were the most common: cis-11-hexadecenal (10.2%), trans-13-octadecenoic acid (9.5%), and 6-Octadecenoic acid, methyl ester, (Z)-(8.8%). The α -glucosidase enzyme was targeted in a docking study to investigate the antidiabetic properties of the 42 phytochemicals found in the essential oil extract. The compound, namely 5.alpha.-Androstan-16-one, showed the highest binding affinities of -8.6 Kcal/mol during the docking screening of the 42 identified phytochemicals against α -glucosidase. These two compounds show potential as competitive α -glucosidase inhibitors. *E. camaldulensis* will be a particularly useful source to improve health and fight communicable and non-communicable diseases. Nonetheless, human evaluations of *E. camaldulensis* safety and effectiveness are necessary, and more well-planned clinical trials are needed to confirm our *in vitro* and *in silico* findings.

Keywords: diseases; medicinal; plant; traditional; protein docking; molecular dynamics

1. Introduction

The prevalence of non-communicable diseases diabetes is increasing at an alarming rate. In 2015, it was predicted that 422 million individuals would develop diabetes mellitus (DM) [1]. By 2035, it is expected that this figure will double [1]. The incidence of diabetes on a global scale is a serious public health issue; it has either caused or aggravated numerous clinical conditions, such as hypertension, heart disease, excessive cholesterol, cancer, and dementia [2].

The need to discover new antimicrobial compounds is being increasingly recognized in this age of antibiotic resistance [3]. There is a growing need for novel chemicals with direct antibacterial or indirect action that enhances the resistance mechanism of microorganisms, since infectious illnesses continue to be a major public health concern. Plants' natural products are crucial to the search for new therapeutic medicines [4].

Plants are employed either directly or indirectly in the composition of 25% of today's medications, many of which are made from medicinal plants [4]. In recent years, the potential for the treatment of numerous diseases with medicinal plants has been a growing [5]. The treatment of diseases from plant products are risk free, less toxic, and inexpensive [6].

Natural products obtained from plants are known to be alternative forms of medicine and have gained a lot of attention. For improvement of health statuses and the treatment of diverse ailments, a great percentage of people all over the world rely on natural products derived from plant parts [7]. As a medical substance, medicinal plants play an essential role in pharmacological research, disease treatment and prevention, and as raw materials for the creation of pharmacologically active products [8].

Pharmacokinetic variables are increasingly being incorporated into drug discovery procedures using computer-based methodologies [9]. A chemical with both a high potency and a favorable chemical absorption, distribution, metabolism, excretion, and toxicity (ADMET) profile is considered

a potential lead compound. Therefore, regardless of their great potency, drugs with unimpressive projected ADMET profiles can be quickly removed from the pool of potential therapeutic candidates [10]. The use of computational approaches in medical synthetic chemistry has become commonplace; however, its application in the study of natural chemicals has not received enough attention.

There are 131 genera and about 5500 species in the Myrtaceae family, all of which are woody trees or shrubs and have essential oils [11]. Several family members are commercially well-known for their therapeutic essential oils [11]. *E. camaldulensis*, which is a species of the Myrtaceae family, is commonly used to treat stomach ailments in Nigeria.

Moreover, a decoction made from the leaves is claimed to be effective against urinary tract infections, respiratory tract infections, and sore throats caused by bacteria. A poultice produced from the leaves is used to treat wounds and sores [12]. The anti-tubercular effect of the essential oils extracted from the leaves has led to their usage in the treatment of lung ailments [12]. With its infusions, one can treat gastrointestinal problems, respiratory problems, halt bleeding, heal cuts and open wounds, and relieve aches and pains in the muscles, joints, and teeth [13]. Bacterial infections and inflammatory-related disorders are traditionally cured with an extract made from the leaves [14]. The plant is extensively utilized in traditional treatments for colds, asthma, diarrhea, dysentery, laryngitis, and sore throats [15]. Previously, there was antimicrobial investigation on *E. camaldulensis* [12,16,17]. Antibiotic-resistant diseases cost approximately up to \$29,069 per patient and can lead to an extended length of treatment. Therefore, there is a need to find cutting-edge, natural, antimicrobial drugs and treatments [14].

The aim of this study is to use various *in vitro* biological models in combination with *in silico* analysis to enhance the current literature. This involves assessing the antioxidant, anti-diabetic, and antibacterial properties alongside specific *in silico* methods to predict the drug-likeness, pharmacokinetic behavior, and binding effectiveness of the identified phytochemicals extracted from *E. camaldulensis* leaves.

2. Materials and methods

2.1. Plant collection and identification

E. camaldulensis leaves samples (Figure 1) were gathered from outdoor areas, field gardens, and backyard gardens; subsequently, herbarium specimens were made. After the verification of the plant's identity by a qualified taxonomist, the plants were donated to the Ahmadu Bello University Herbarium in Zaria with the following assign voucher number: ABU02510. The World Flora Online (WFO) <https://www.worldfloraonline.org/> was utilized to authenticate the species name.



Figure 1. The leaves of *Eucalyptus camaldulensis* Dehnh.

2.2. Extraction of plant samples

The leaves were washed under running water to get rid of any remaining dirt, stains, or latex. A grinding machine was employed to pulverize the dehydrated samples into a fine powder. The powdered plant samples were quantified by weighing 100 g of the sample. The Soxhlet technique was used to extract ethanol and an aqueous layer from the plant leaves.

A Whitman No. 1 filter was used to filter the extraction's result. Both the ethanol and aqueous plant leaf samples were crudely extracted using the E-Z-2-Elite evaporation apparatus. For the ethanol and aqueous extracts, the solvent pressure was set to 72 and 300, respectively, and the vacuum was set to 40 °C [18]. The extracts were dried in a refrigerated vacuum oven at 40 °C until they reached a uniform mass, after which they were concentrated with a rotary evaporator and weighed with an electronic balance [19]. The weight of the crude yield is derived by the following simple calculation: $Yield \% = Extraction\ yield\ (\%) = F1/F2 \times 100$, where F1 is the mass of the crude extract and F2 is the mass of the sample [20].

2.3. Essential oil distillation

Freshly cut *E. camaldulensis* leaves were extracted in a Clevenger device under reflux for 4 hours. Then, the resulting essential oil (EO) was extracted with dichloromethane, the organic phase was separated and dried with anhydrous sodium sulphate, filtered, and stored in an airtight flask at a low temperature (−10 °C) [21]. This method was carried out in triplicate and the percent yield was computed in relation to the dried mass of the initial sample.

2.4. 6.4.1.2 1, 1-Diphenyl-2-Picryl Hydrazyl (DPPH) radical scavenging activity

Seven different concentrations of ethanol, aqueous, and EO of the leaves were subjected to a 100 g mL⁻¹ (0.004% w/v) DPPH methanol solution to determine its effect. For 30 minutes, the solution was

allowed to sit undisturbed at room temperature and without light. Comparisons were made using quercetin as a standard [22]. The calculation for the radical scavenging activity is as follows:

$$\% \text{ Inhibition} = [(B_0 - B_1) / B_0] \times 100$$

where B1 is the sample absorbance (517 nm) and B0 is the control absorbance (517 nm) reaction.

2.5. Ferric reducing antioxidant power (FRAP) assay

A mixture of acetate buffer (B, 300 mM), 2,4,6-tri (2-pyridyl) -S-triazine (TPTZ, 10 mM) in HCl (40 mM), and iron chloride (FeCl₃, 20 mM) were heated in a water bath for 10 minutes at 37 degrees Celsius. Following a 30-minute incubation at room temperature in the dark, 285 L of a FRAP working solution (100 µg/g mL concentrations) was added to 15 µL of ethanol, aqueous, or EO (100%) extracts of the leaf samples [22].

2.6. α -glucosidase inhibition assay

50 µL of 0.1 M phosphate buffer (pH 7.0) was combined with 10 µL of the ethanol, aqueous, or EO extracts of the leaves at 100 µg/mL. 25 L of α -glucosidase (Sigma Aldrich) in buffer (0.2 U/mL) was placed onto a well plate to initiate the reaction. A 25 µL sample of 0.5 mM 4-nitrophenyl alpha-Dglucopyranoside (pNPG) substrate was added to complete the reaction, which was then incubated for an additional 30 minutes at 37 °C [23]. The process was stopped by introducing 100 µL of a 0.2 M sodium carbonate solution. Acarbose at 100 µg/mL was used as a positive control. The absorbance was determined at 410 nm. The percent inhibition was calculated using the following formula:

$$\text{Inhibition (\%)} = [\text{Control abs} - \text{sample abs}] / \text{control abs} \times 100$$

3. Antimicrobial evaluation

3.1. Test organisms

Gram-positive *Pseudomonas aeruginosa* and Gram-negative *Staphylococcus aureus* bacteria were provided by the biology department of Tishk International University. Mueller Hinton agar plates were streaked with the microbial stock cultures using an inoculation loop, and then the plates were incubated at 37 °C overnight. The following day, they were subcultured again until a new colony was established. After that, they were injected with Mueller Hinton broth and allowed to incubate at 200 rpm overnight [24].

3.2. Disk diffusion evaluation

Microbial inoculums containing 1.106 (CFU)/mL were seeded onto 200 µL solidified Mueller-Hinson plates. The plant component (ethanolic, aqueous, and EO) extracts were impregnated with 20 µL of 4000 µg/mL on Whatman No. 1 filter paper discs (6 mm). Using sterile forceps, the impregnated disk was positioned on the plates. The plates were incubated at 37 °C for 24 hours [24].

3.3. Essential oil identification

Components of the EOs were analysed by means of gas chromatography linked to mass spectrometry (GC-MS, Shimadzu/QP2010) with an OV-5 bonded capillary column (30 m 0.25 mm 0.25 m film thickness). The propellant gas was helium, and the flow rate was 1 mL/min. Temperatures of 220 and 240 °C were reached in the injector and detector, respectively. 1.0 µL was injected at a split ratio of 1: 20. The oven temperature was set to gradually increase from 60 °C to 240 °C at a rate of 3 °C/min with 1 min hold. The collected pieces had velocities ranging from 40 to 650 m/z and an electron impact energy of 70 eV [21].

3.4. Statistical analysis

The experiments were performed in a completely randomized manner, with three replicates of each treatment, and the statistical analyses were performed using the Statistical Analysis System (SAS) for data analysis (University version 9.4). After performing a one-way repeated-measures analysis of variance (ANOVA) [25], a post-hoc test, namely Duncan's multiple range test, was employed to evaluate if there were any statistically significant differences between the group means at the $p \leq 0.05$ level.

3.5. Molecular docking of α -glucosidase

Antidiabetic properties of the phytochemicals isolated from *E. camaldulensis* were investigated in a docking study against the α -glucosidase enzyme (Protein Data Bank (PDB): 3A4A). The selection of the 3A4A PDB structure was made considering several factors, including its crystallization with an inhibitor to compare with docked ligands, a resolution of less than 2 Å, and the absence of mutations. The protein was obtained and downloaded as a PDB file from the following: <https://www.rcsb.org/>. Chimera software tools [26] were used to remove the native ligand present in the PDB structure of the protein.

The 1D structures of the isolated phytochemicals and the four controls including the native inhibitor, alpha-D-glucopyranose, were retrieved from the PubChem Search database as strings of canonical smiles. To facilitate the analysis, the smile sequences were converted into 3D PDB files using a web server known as CORINA, <https://demos.mn-am.com/corina.html>.

The CB-Dock server automatically optimizes the ligand input files as reported by [27]. CB-Dock is a docking tool for protein-ligand interactions that automatically detects the binding sites, determines their center and size, adjusts the docking box dimensions based on the query ligands, and subsequently conducts molecular docking using the AutoDock Vina software, v1.2.5 [28]. The docking process consists of three steps: Search Cavities, View Results, and BlindDock. The active site parameters for docking included a Cavity Volume of 2996 Å³, with the center coordinates of X = 15, Y = -14, and Z = 16. The generated poses were evaluated and visualized using the CB-Dock server and Chimera software tools.

The inhibition constant (K_i) was calculated using the following formula: $K_i = \exp(\Delta G/RT)$, where ΔG is the binding energy, R is the universal gas constant (1.985×10^{-3} kcal mol⁻¹ K⁻¹), and T is the temperature (298.15 K).

3.6. Molecular dynamics (MD) simulation of α -glucosidase

A molecular dynamics (MD) simulation was performed using the CABS Flex 2.0 server [29] for α -glucosidase (without ligands) and α -glucosidase-5.alpha.-androstan-16-one complex to calculate the root mean square fluctuation (RMSF) values. The parameters used were as follows: Time, 10 ns; Mode, SS2; Interval, 3; Global weight, 1.0; Number of cycles, 50; Cycles between trajectory frames, 50; Simulation temperature, 1.4; and Random number generator seed, 5546.

3.7. Drug-likeness properties

The SMILES strings of the 5.alpha.-Androstan-16-one compound were obtained from PubChem (<http://pubchem.ncbi.nlm.nih.gov/>). Next, we calculated the drug-likeness parameters of the analyzed compound using the SwissADME online webserver (<http://www.swissadme.ch/index.php>). The bioactivity score for an enzyme inhibitor was determined through the utilization of the Molinspiration server located at <http://www.molinspiration.com/cgi-bin/properties>. The prediction of hepatotoxicity toxicity was conducted using pkCSM, which is a server that predicts the toxicity of small molecules, <https://biosig.lab.uq.edu.au/pkcsm/prediction>.

4. Results

4.1. Extraction yield

The aqueous extract of *Eucalyptus camaldulensis* leaves had a greater yield of 0.87% compared to the ethanol extract and EO, which had yields of 0.65% and 0.48%, respectively (Figure 2).

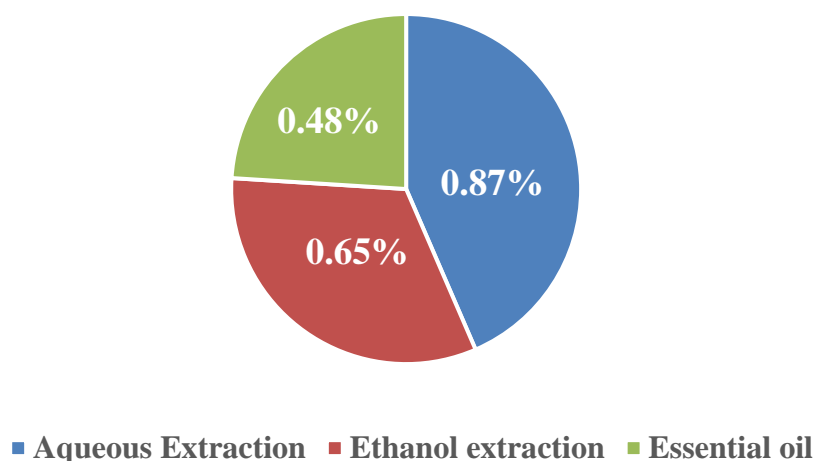


Figure 2. Extraction yield of ethanol, aqueous and essential oil.

4.2. Antioxidant, α -glucosidase and antimicrobial Activities of *E. camaldulensis* leaves

Table 1 displays the inhibitory effects of the ethanol, aqueous, and EO extracts of *E. camaldulensis* leaves using the DPPH radical scavenging method. The highest inhibition was recorded

from the EO at 84 % (Table 1 and Figure 3). The highest capacity to convert Fe^{3+} to Fe^{2+} was noted for the aqueous leaves extract, even when compared to the standard used (Figure 4). The result exhibits a significant difference among the examined treatments. The principal enzyme in charge of catalysing the final stage of carbohydrate digestion is α -glucosidase. The highest level of α -glucosidase activity for the leaf EO was reported to have an inhibitory value of 78 % (Table 1). The tested extract demonstrated a substantial zone of inhibition against the tested strains of *Staphylococcus aureus* and *Pseudomonas aeruginosa*. The EO exhibited the highest zone of inhibition at 12 mm and 14 mm for *Staphylococcus aureus* and *Pseudomonas aeruginosa*, respectively. These values were greater than the zone of inhibition observed for ampicillin at 9 mm and 6 mm for *S. aureus* and *P. aeruginosa*, respectively (Figure 5). A statistically significant difference was found between the treatments at $p \leq 0.05$. Due to the significant activity of the EO, it underwent further examination of its chemical makeup using GCMS.

Table 1. Antioxidant, α -glucosidase and antimicrobial activities of *E. camaldulensis* leaves.

S/N	Plant part/extract	% of inhibition of DPPH	FRAP Fe^{2+} (mmol/g)	% of inhibition of α -glucosidase	Zone of inhibition <i>Staphylococcus aureus</i> (mm)	Zone of inhibition <i>Pseudomonas aeruginosa</i> (mm)
1	Ethanol Leaves	75.1 ± 1.0^b	12.9 ± 2^c	60 ± 0.2^c	$10^{b,c}$	8^b
2	Aqueous Leaves	$69.3 \pm 03^{c,d}$	10.4 ± 4^d	63 ± 1.0^b	6^d	$6^{c,d}$
3	Essential oil	84.01 ± 01^a	20.1 ± 1^a	78 ± 2.1^a	12^a	14^a
4	Quercetin/ Acarbose	70.04 ± 2.0^c	15.8 ± 1^b	54 ± 0.1^d		
5	Ampicillin (10 μg)				9^c	6^d

Note: The numbers represent the means and standard deviations of three separate experiments, each of which was carried out three times. Vertically similar alphabets do not statistically differ at the $p \leq 0.05$ level.

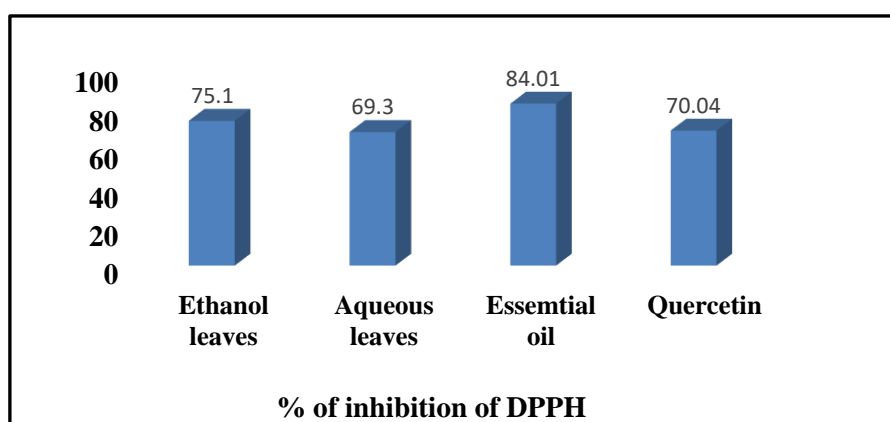


Figure 3. Percentage of DPPH radical scavenging activities.

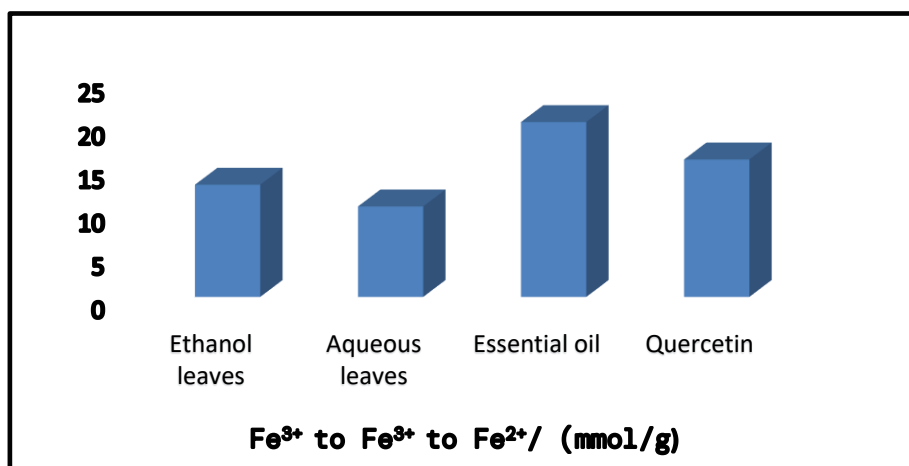


Figure 4. Bar graph of FRAP showing the extract capacity to convert Fe^{3+} to Fe^{2+} .

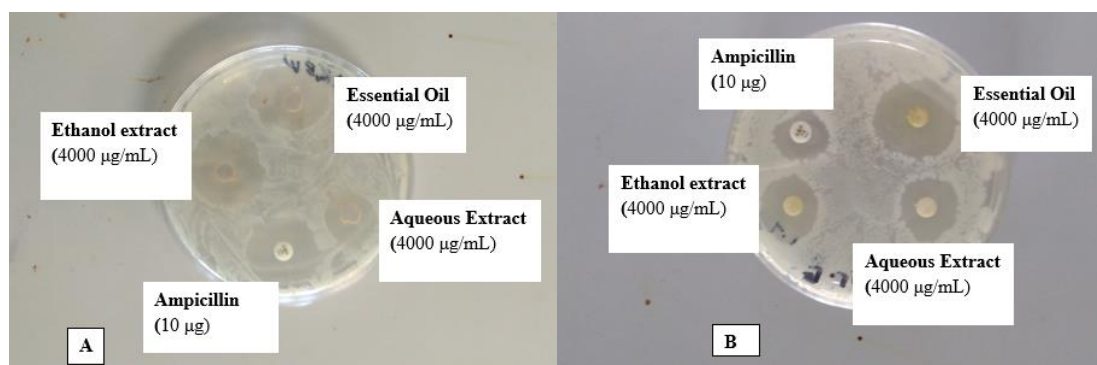
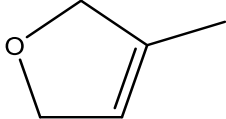
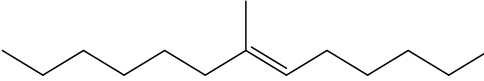
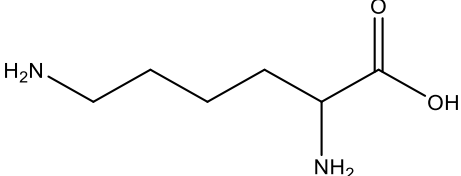
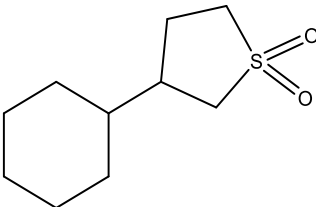
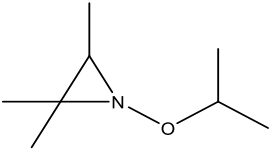
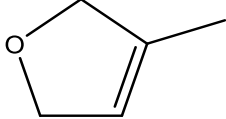


Figure 5. Leaves essential oil activity against (A) *Staphylococcus aureus* and B *Pseudomonas aeruginosa*.

4.3. Chemical composition

Table 2 exhibits the spectra of the EOs identified components (mass spectrum of each compound of the EO are presented in Supplementary Table S2). The EO was broken down into its 42 constituent compounds with 99.9% of the EO (Figure 6). There was a dominance of cis-11-Hexadecenal (10.2%), trans-13-Octadecenoic acid (9.5%), and 6-Octadecenoic acid, methyl ester, (Z)- (8.8%), with the rest having 7 to 0.1%, respectively (Table 2).

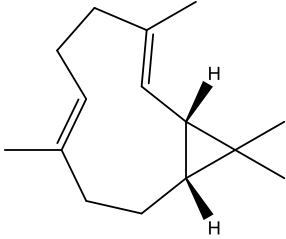
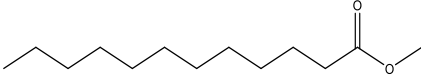
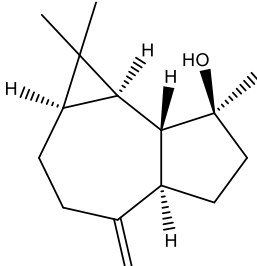
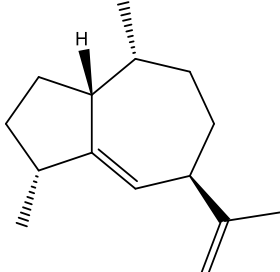
Table 2. Essential oil constituents of *Eucalyptus camaldulensis*.

S/N	RT	Area	Compound	Molecular structure
1	6.9295	0.5058	Furan, 2,5-dihydro-3-methyl-	
2	7.6833	1.4124	6-Tridecene, 7-methyl-	
3	8.1449	1.147	dl-Lysine	
4	8.4441	1.1377	3-Cyclohexylthiolane,S,S-dioxide	
5	8.6201	0.9649	1-Isopropoxy-2,2,3-trimethylaziridine	
6	8.7722	0.6063	Furan, 2,5-dihydro-3-methyl-	

Continued on next page

S/N	RT	Area	Compound	Molecular structure
7	8.8871	0.982	1H-Cyclopropa[a]naphthalene, 1a,2,3,5,6,7,7a,7b-octahydro-1,1,7,7a-tetramethyl-, [1aR-(1a.alpha.,7.alpha.,7a.alpha.,7b.alpha.)]-	
8	9.068	8.0481	Aromandendrene	
9	9.5046	4.099	Alloaromadendrene	
10	9.7889	1.7229	5.alpha.-Androstan-16-one	

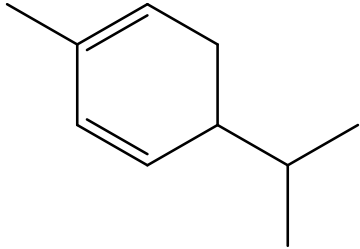
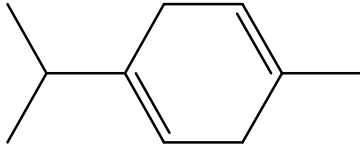
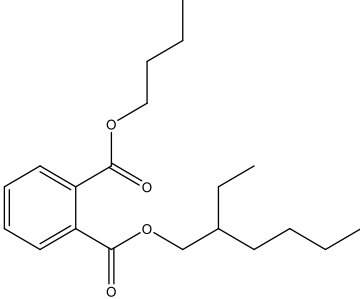
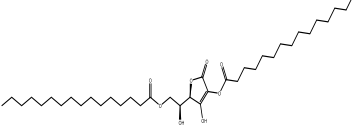
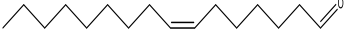
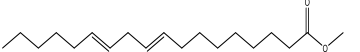
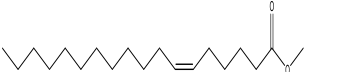
Continued on next page

S/N	RT	Area	Compound	Molecular structure
11	10.329	2.5538	(1S,2E,6E,10R)-3,7,11,11-Tetramethylbicyclo[8.1.0]undeca-2,6-diene	
12	11.2245	0.3508	Dodecanoic acid, methyl ester	
13	11.8237	0.2395	1-Methylene-2b-hydroxymethyl-3,3-dimethyl-4b-(3-methylbut-2-enyl)-cyclohexane	
14	12.153	0.5436	1H-Cycloprop[e]azulen-7-ol, decahydro-1,1,7-trimethyl-4-methylene-, [1ar-(1a.alpha.,4a.alpha.,7b.alpha.)]-	
15	12.3177	3.3133	Azulene, 1,2,3,3a,4,5,6,7-octahydro-1,4-dimethyl-7-(1-methylethenyl)-, [1R-(1.alpha.,3a.beta.,4.alpha.,7.beta.)]-	

Continued on next page

S/N	RT	Area	Compound	Molecular structure
16	12.6917	0.8741	Naphthalene, decahydro-4a-methyl-1-methylene-7-(1-methylethenyl)-, [4aR-(4a.alpha.,7.alpha.,8a.beta.)]-	
17	12.9604	0.2569	1-Tetradecene	
18	13.1784	1.1556	2-Naphthalenemethanol, 2,3,4,4a,5,6,7,8-octahydro-.alpha.,.alpha.,4a,8-tetramethyl-, [2R-(2.alpha.,4a.beta.,8.beta.)]-	
19	13.9033	1.1754	3-Tetradecynoic acid	
20	14.1865	0.5571	Methyl 10-oxo-8-decenoate	
21	14.9428	0.1751	9-Hexadecenoic acid, octadecyl ester	
22	15.4386	2.6144	cis-Z-alpha-Bisabolene epoxide	

Continued on next page

S/N	RT	Area	Compound	Molecular structure
23	17.0159	0.604	Alpha-Phellandrene	
24	17.3444	0.1292	Gamma-Terpinene	
25	19.8713	1.4356	13-Octadecenal, (Z)-	
26	20.0676	1.31	1,2-Benzenedicarboxylic acid, butyl 2-ethylhexyl ester	
27	21.5497	1.3177	1-(+)-Ascorbic acid 2,6-dihexadecanoate	
28	21.9975	1.6346	7-Hexadecenal, (Z)-	
29	22.9324	7.7147	9,12-Octadecadienoic acid, methyl ester	
30	23.0931	8.8599	6-Octadecenoic acid, methyl ester, (Z)-	

Continued on next page

S/N	RT	Area	Compound	Molecular structure
31	23.4822	3.9623	9-Hexadecenoic acid	
32	23.6908	1.2546	Methyl stearate	
33	24.342	1.8422	1,19-Eicosadiene	
34	24.5097	1.5373	9-Tetradecenal, (Z)-	
35	30.3053	0.5913	15-Hydroxypentadecanoic acid	
36	31.6831	0.7238	E-9-Tetradecenal	
37	32.9886	10.3582	13-octadecadienol	
38	33.1566	2.9289	cis-Vaccenic acid	
39	33.3425	4.5968	trans-13-Octadecenoic acid	
40	35.8604	0.8797	13-octadecadienol	
41	35.971	1.2193	Eicosane	
42	38.4646	10.2357	cis-11-Hexadecenal	

Note: S/N = Serial number, RT = Retention time.

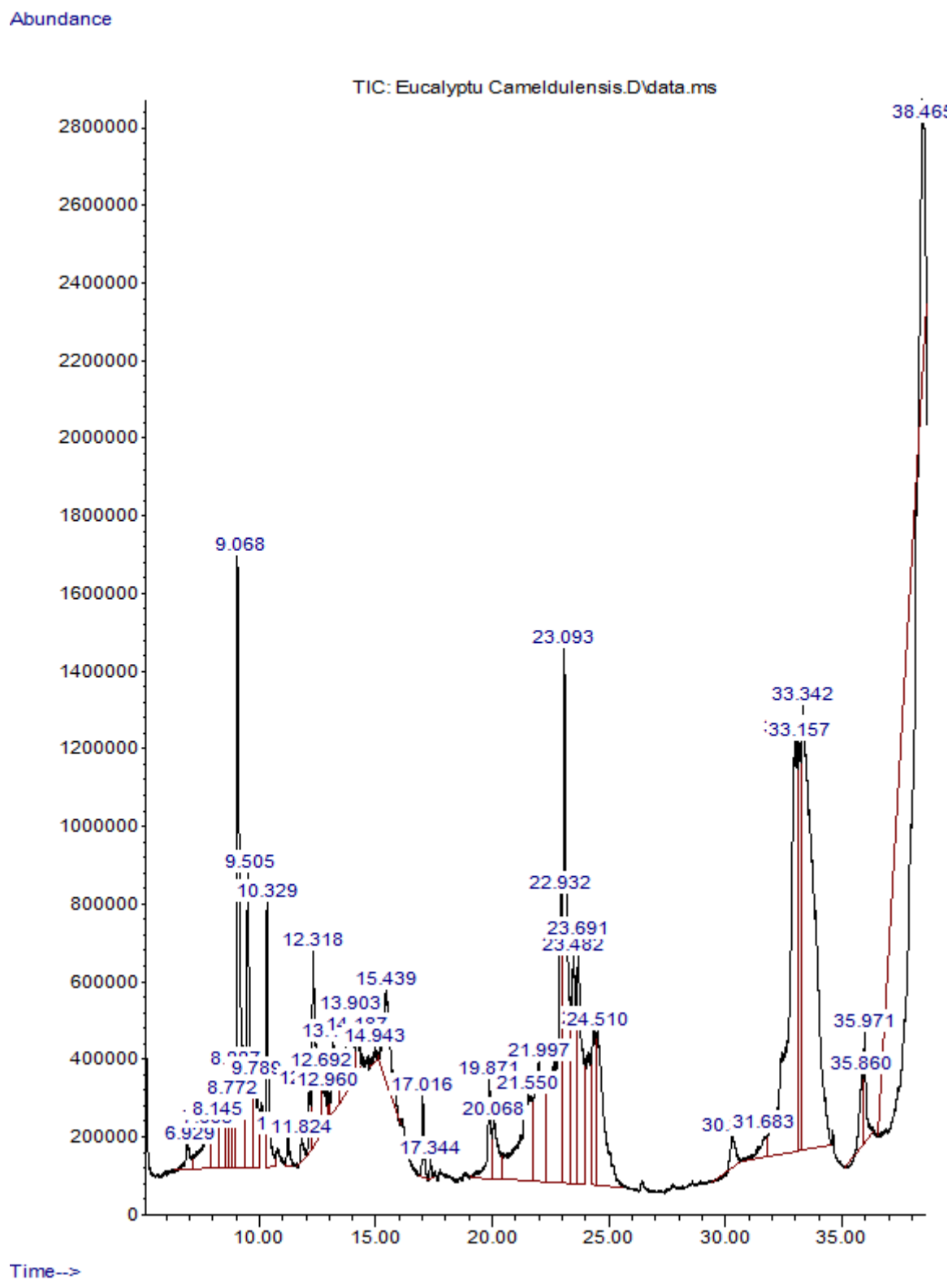


Figure 6. Chromatogram of essential oil of *E. camaldulensis* leaves.

4.4. Molecular docking analysis

The results of the *in vitro* experiment showed a high possibility that the leaf extracts of *E. camaldulensis* inhibited the α -glucosidase enzyme. This motivated us to evaluate the potential inhibitory role of the phytochemicals of *E. camaldulensis* and to identify the binding affinity value for each compound. It is crucial to validate the docking protocol to ensure the precision of the docking process. Therefore, the co-crystallized ligand, namely alpha-D-glucopyranose, was eliminated from the α -glucosidase PDB structure. Subsequently, a new alpha-D-glucopyranose was generated by the CORINA server as described in the methods and used to redock the PDB structure. The CABS Flex 2.0 server effectively re-docked the newly generated ligand into the active site of α -glucosidase (Figure 7), resulting in interactions similar to those observed in the original structure. Despite using blind docking and not specifying the active site, a good match between the docking structure and the original PDB structure was obtained, indicating the docking accuracy.

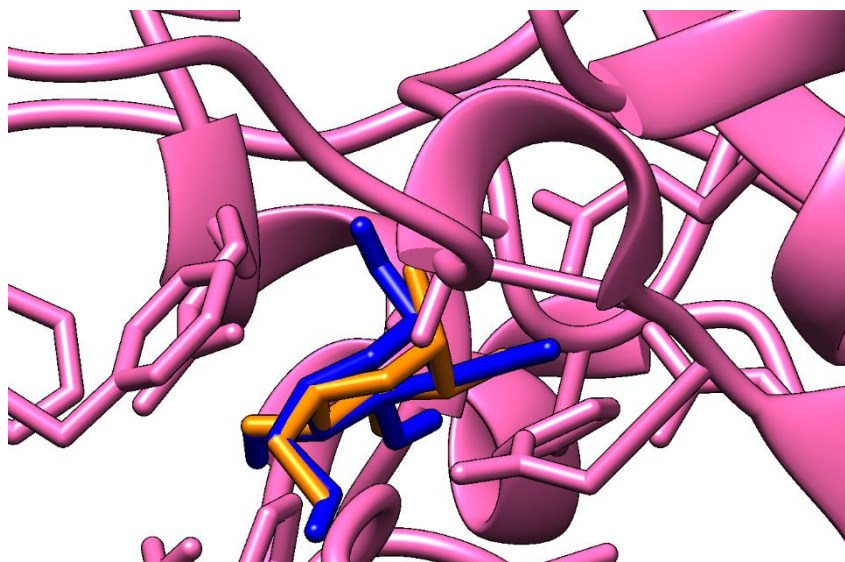


Figure 7. The validation of the docking protocol. α -glucosidase enzyme (pink), along with the redocked generated ligand (blue) and the native ligand, alpha-D-glucopyranose (orange), are presented.

The phytochemicals isolated from the *E. camaldulensis* leaves (Table 2) were subjected to docking studies to estimate their antidiabetic effects against α -glucosidase, as illustrated in Table 3 and Figure 8. Additionally, the inhibition constant (K_i) was calculated based on the binding energy (ΔG) using the formula mentioned in the methods section. The results of the docking analysis revealed that the 5.alpha.-Androstan-16-one compound exhibited significant binding affinities towards α -glucosidase compared to other phytochemicals. The two compounds mentioned above produced higher binding affinities compared to the controls, with scores of -8.6 and -8.5 Kcal/mol, respectively, as presented in Table 3. Quercetin exhibited the highest binding affinity among the five controls, with a score of -8.6 Kcal/mol. This score is comparable to the scores obtained by 5.alpha.-Androstan-16-one. A further analysis was conducted on 5.alpha.-Androstan-16-one due to its strong interaction with α -glucosidase. The analysis showed that the compound could interact with the enzyme via 11 amino

acids (TYR158, GLN279, PHE303, ASP307, PRO312, LEU313, PHE314, ARG315, ASP352, GLN353, GLU411, and ARG442), as shown in Figure 8.

Table 3. The docking scores and Inhibition constant (Ki) of examined compounds against α -glucosidase.

Compound	PubChem CID	Docking Score	Inhibition constant Ki (μ M)
alpha-D-glucopyranose (Native Inhibitor)	79025	-6.2	27.5
Quercetin	5280343	-8.6	0.5
Acarbose	41774	-8.3	0.8
Miglitol	441314	-5.8	55.4
Voglibose	444020	-6.4	20.3
Phytochemicals of <i>Eucalyptus camaldulensis</i> that gave best scores			
5.alpha.-Androstan-16-one	13963520	-8.6	0.5

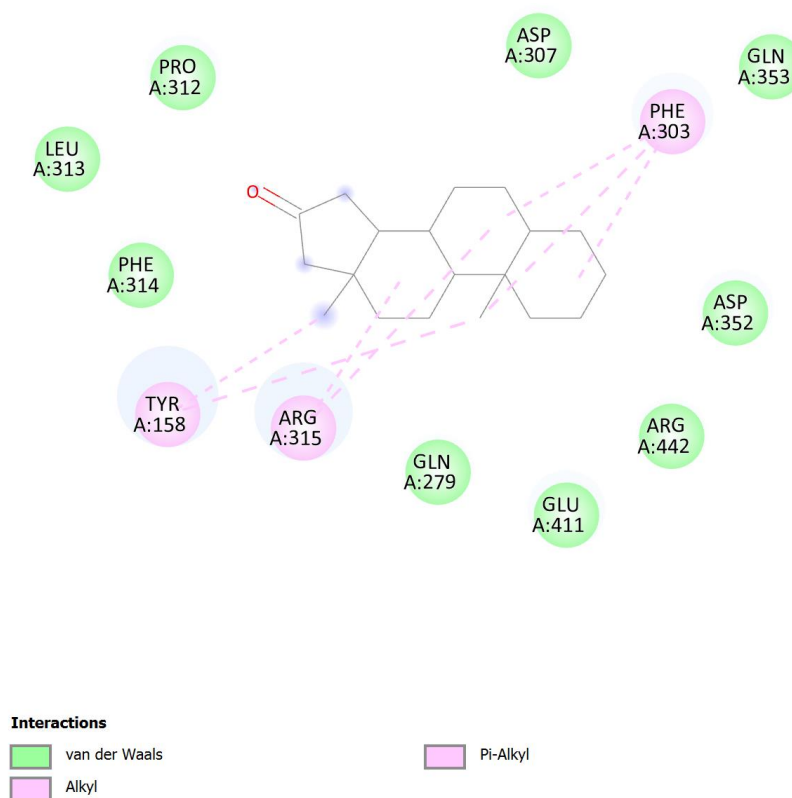


Figure 8. The amino acids located in the active site of α -glucosidase interact with 5.alpha.-Androstan-16-one compound.

4.5. Molecular dynamics analysis

A MD simulation of 10 ns was conducted utilizing the CABS-flex 2.0 server in order to determine the RMSF values for the α -glucosidase-5.alpha.-Androstan-16-one complex, as shown in Figure 9.

The fluctuation of atoms throughout the simulations provides insight into the flexibility and stability of various protein residues. A higher RMSF value for the residues suggests an increased flexibility of the amino acid, while lower fluctuations suggest restricted movements during the MD simulation. The fluctuation in the complex was found in the acceptable range between 1 and 3 Å, indicating that there is no binding effect of 5 α -androstan-16-one on the α -glucosidase enzyme. The LYS127, ALA145, and SER574 residues exhibited fluctuations higher than 3 Å; however, these exceptions were found outside the active site and did not impact the binding to the ligands. In multiple regions within the active site, 5 α -androstan-16-one enhanced the rigidity of the enzyme and improved the stability of binding, as shown in the dashed line box.

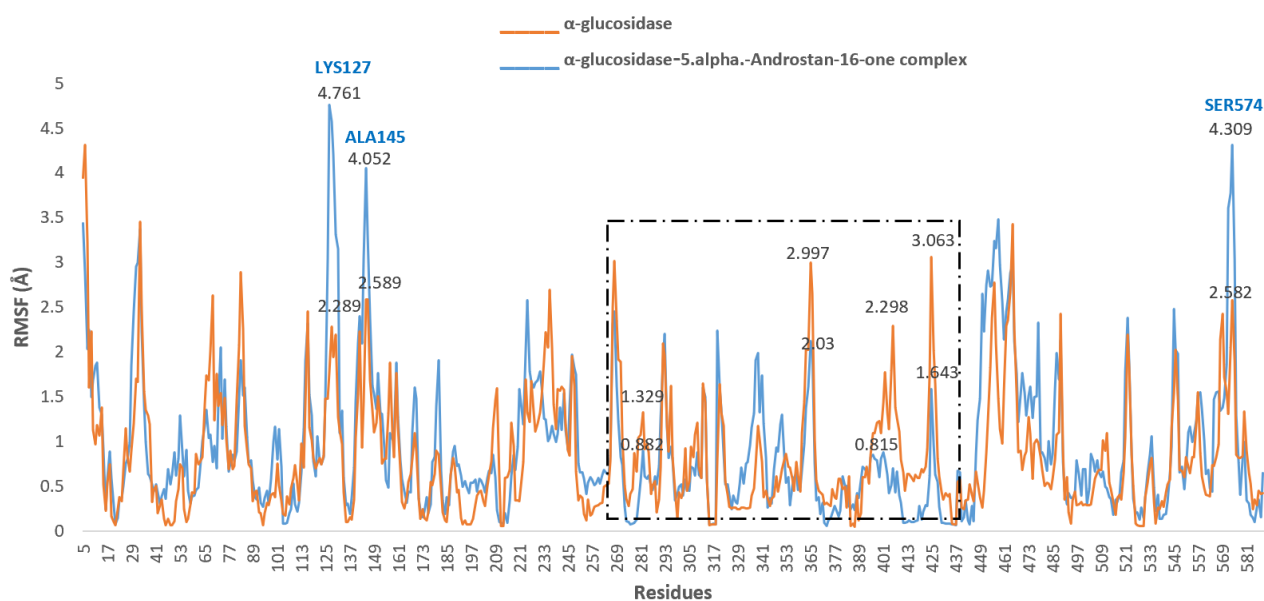


Figure 9. The RMSF plot (Å) of α -glucosidase enzyme (orange) and 5.alpha.-Androstan-16-one complex (blue). The amino RMSF plots are constructed from the backbone C α atoms.

4.6. Assessment of ADMET

The promising phytochemical, namely 5.alpha.-Androstan-16-one, underwent evaluation to determine its potential as a drug that can be taken orally by humans, in accordance with Lipinski's rule of five (RO5), and was assessed for the ADMET parameters. The compound successfully met Lipinski's rule of five, with only one violation observed due to MLOGP > 4.15. The compound showed a high gastrointestinal absorption. In regard to its solubility, 5.alpha.-Androstan-16-one exhibited a moderate solubility. The compound received enzyme inhibitor scores of 0.34, with neither showing any hepatotoxicity.

5. Discussion

The yield varied greatly according to the extraction solvents (Table 1). The solvent's ability to extract more compounds from the samples may account for the high yield found in the aqueous extracts.

The findings are consistent with Poojary et al. [30], who observed a significant yield of extract from the root and bark using an aqueous extraction method, with a reported yield of 10.43%. The extraction process, solvent type, chemical type, and metabolite polarity were the main factors that influenced the yield extract variance between the medicinal plant parts [18]. Choosing the appropriate extraction solvent is significant to obtain a higher yield of compounds. A diverse number of solvents, such as aqueous diethyl ether, ethanol, hexane, methanol, and chloroform, has previously been used to extract bioactive substances in plant parts [31]. Each bioactive compound has a different solubility in specific solvents. Therefore, the correct choice of organic solvent is significant to recover different forms of compounds. It is necessary to select solvents that are safe for use in the industrial production processes.

In terms of the radical scavenging activity, the high activity of the EO might be because the plant is known to be highly aromatic. The Fe^{3+} complex in tripyridyl-triazine (TPTZ) is reduced to the Fe^{2+} complex, Fe^{2+} (TPTZ), which results in a blue colour shift in this process [32]. When compared to their scavenging activity, the antioxidant content of the ethanol, aqueous, and EO extracts did not significantly differ based on their reduction potential. The action of each extract established in the various solvents is explained by the presence of a specific component, such as a hydroxyl group, a methoxyl group, phenolic compounds, flavonoids compounds, or other structures that may be present [18]. The number and type of phytochemical compounds found in the plant extract are solely responsible of the environmental condition [33]. Possible explanations for the observed discrepancy between the DPPH and FRAP assays include differences in the actions or responses of the compounds toward the assay. Multiple studies have conclusively established the importance of oxidative stress in the development and progression of DM [34].

Therefore, antioxidant compounds such as plant polyphenols have been proposed as potential tools in the fight against and the treatment of this disease. The findings of the DPPH and FRAP assays for antioxidant activity led us to infer that the EO extracted from the leaves had the maximum antioxidant activity. More work is needed to isolate the compounds in the leaves' EOs responsible for its antioxidant properties before it can be used therapeutically. The beneficial effects on glucose homeostasis can be shown in DM patients when these enzymes are inhibited, as less oligosaccharide and disaccharide hydrolysis occurs [35]. Therefore, blocking the α -glucosidase enzyme is a crucial part of diabetes management [36].

All the extracts that showed varying levels of activity against the bacterial strains were tested. An increase in activity was observed with increasing concentrations of both the ethanol and aqueous extract and EO (Table 1). The EO demonstrated a superior action compared to the ethanol and aqueous extracts, as well as the ampicillin standard (Table 1). The results were consistent with the findings of Sabo et al. [13], where the EO derived from *E. camaldulensis* exhibited an antimicrobial activity against a wide range of Gram-positive bacteria (0.07–1.1%) and Gram-negative bacteria (0.01–3.2%). Consequently, the treatment of bacterial infections necessitated the administration of larger quantities of the oil [16].

E. camaldulensis leaves have long been recommended by traditional herbalists as a potent diabetic treatment, and recent scientific studies have confirmed these assertions. One of the reasons for the high activity of the leaves extracts might be because the secondary metabolites are first produced in the leaves before being transferred to the rest of the plant. The plant's secondary metabolites have crucial roles in disease resistance, pollination, and adaptability. Many aspects of a man's daily life make use of the secondary metabolites produced by the plant's parts. It's common knowledge that these chemical by-products, treated or not, have several biological applications [37].

Forty-two non-polar compounds identified for the EO of the leaves might be responsible for the high antioxidant and alpha glucosidase inhibition activities. Increasing insulin secretion and pancreatic-cell regeneration are two ways in which the following substances have been found to have anti-diabetic effects [38]. Antioxidant and anti-diabetic effects have been observed in secondary metabolites and bioactive phyto-constituents discovered by GC/MS in a wide range of plants [35]. The chemical composition revealed the presence of 41 compounds with a diverse array of pharmacological activities. Compounds such as Aromadendrin have been recorded to possess numerous pharmacological properties, such as anti-inflammatory, antioxidant, and anti-diabetic attributes [39]. Famous for its anti-inflammatory qualities in treating peptic ulcers, azulene also has anti-tumor and anti-retroviral activities against HIV-1, antimicrobial qualities, including antimicrobial photodynamic therapy, and antifungal qualities. Additionally, it has antineoplastic effects in fighting leukemia [40]. Studies revealed that 9-hexadecenoic acid and trans-13-octadecenoic acid had possible anti-inflammatory properties, suggesting a viable substitute for treating a variety of ailments linked to pain and inflammation [41,42].

The results of the MD analysis revealed that the majority of phytochemicals found in *E. camaldulensis* exhibited a binding score higher than -6.2 Kcal/mol, where the score was obtained by the native inhibitor, as shown in Supplementary Table S1. Typically, in drug design, the primary criteria for selecting potential candidates involves binding free energy values that are usually lower than -6.0 kcal/mol [43].

The strong inhibition observed by the *in silico* study aligns with the *in vitro* findings, where the *E. camaldulensis* extracts demonstrated inhibition of α -glucosidase activity at a percent inhibition ranging from 60-78 %, which is comparable to the percent inhibition of Quercetin at 84 %. The selection of Quercetin as a positive control in the docking study was based on its use in the *in vitro* study. Upon comparing the level of inhibition exhibited by Quercetin against α -glucosidase in both studies, it was observed that it achieved a significant degree of inhibition nearly equivalent to the inhibition observed for most of the phytochemicals, particularly the 5.alpha.-Androstan-16-one compound. Our *in silico* results showed that the compound 5.alpha.-Androstan-16-one displayed a significant inhibitory activity, with a binding affinity of -8.6 Kcal/mol. Interestingly, these scores are consistent with the binding affinity of Quercetin, which recorded -8.6 kcal/mol. Three residues—TYR158, PHE303, and ARG315—formed non-bond pi-alkyl interactions with 5.alpha.-Androstan-16-one. The pi-alkyl interaction was found to improve the hydrophobic interaction of the ligand in the binding pocket of the receptor, ultimately enhancing its affinity [44]. The strong binding affinity seen in the α -glucosidase-5.alpha.-Androstan-16-one complex may be explained by the presence of pi-alkyl interactions. The inhibition constant (K_i) of 5.alpha.-Androstan-16-one showed the lowest value of 0.5 μ M, which is similar to that obtained by 0.5 μ M Quercetin. It is known that the lower the K_i value, the greater the drug's efficacy [45]. No previous studies were found in the literature that examined the inhibitory activity of 5.alpha.-Androstan-16-one against α -glucosidase.

The MD simulation carried out on the α -glucosidase-5.alpha.-Androstan-16-one complex revealed that the RMSF fluctuation fell within the acceptable range of 1 to 3 Å. This range is considered as the acceptable RMSF criterion to determine protein stability [46]. The results from the MD analysis further demonstrated that the interaction with 5.alpha.-Androstan-16-one led to the enhanced rigidity and stability of α -glucosidase, as evidenced by the reduced RMSF values in various areas of the active site. The correlation between the lower RMSF values and enhanced protein stability was documented by [47]. The terminals of the complex exhibited some high fluctuations, which is a

phenomenon that is frequently observed in proteins [48]. The protein termini are often found on the surface of proteins rather than buried in the core, which contributes to the flexibility of the protein terminals [49].

Drugs such as acarbose, miglitol, and voglibose, which were approved by the FDA, frequently cause stomach-related side effects that hinder their use. As a result, the quest for novel, more potent medications with reduced adverse reactions and lower expenses continues to be a focus of research [50]. In a recent study, 5 α -androstan-16-one showed a stronger competitive inhibition against α -glucosidase compared to FDA-approved diabetes drugs. This natural compound can be a promising diabetic medication with no or fewer side effects compared to those that are usually present in synthetic drugs. In general, the present study revealed that *E. camaldulensis* leaves exhibited a wide range of metabolites that significantly played a role in their antioxidant, anti-diabetic, and antimicrobial potential through unknown mechanisms. The study laid a foundation for pharmacological studies on *E. camaldulensis*. The study suggests that the leaves could be used to make herbal treatments for diabetic people and infectious diseases.

6. Conclusions and recommendation

The findings demonstrated that *E. camaldulensis* has a high antioxidant capacity caused by free radicals and FRAP. Furthermore, *E. camaldulensis* leaves inhibited α -glucosidase at 78 ± 2.1 %. Based on a GCMS analysis, the following chemicals were found to be dominant: cis-11-hexadecenal (10.2%), trans-13-octadecenoic acid (9.5%), and 6-Octadecenoic acid, methyl ester, (Z)- (8.8%). The compound 5.alpha.-Androstan-16-one exhibited a greater competitive inhibition of α -glucosidase compared to FDA-approved antidiabetic medications such as Acarbose, Miglitol, and Voglibose. 5.alpha.-Androstan-16-one has the potential to serve as an effective treatment for diabetes, offering minimal or no side effects that are commonly associated with synthetic medications. The study suggests that the leaves could be used to make herbal treatments for diabetic people. In order to corroborate our *in silico* findings, further *in vitro* and *in vivo* studies are necessary.

Use of AI tools declaration

The authors declare that they have not used Artificial Intelligence (AI) tools in the creation of this article.

Conflict of interest

The authors declare no conflicts of interest.

Author contributions

Conceptualizations: AM Dogara. Experimental analysis: SW Bradosty, SW Hamad, SH Bapir, TK Anwar and AM Dogara. in-silico: AA Al-Zahrani. All authors contributed to the drafting of the initial draft and all authors read and approved the final draft.

References

1. Smolen JS, Burmester GR, Combeet B (2016) NCD risk factor collaboration (NCD-RisC). worldwide trends in diabetes since 1980: a pooled analysis of 751 population-based studies with 4· 4 million participants. *Lancet* 387: 1513–1530. [https://doi.org/10.1016/S0140-6736\(16\)32060-8](https://doi.org/10.1016/S0140-6736(16)32060-8)
2. Eltamany EE, Nafie MS, Khodeer DM, et al. (2020) Rubia tinctorum root extracts: chemical profile and management of type II diabetes mellitus. *RSC Adv* 10: 24159–24168. <https://doi.org/10.1039/D0RA03442H>
3. Pérez Zamora CM, Torres CA, Nuñez MB (2018) Antimicrobial activity and chemical composition of essential oils from *Verbenaceae* species growing in South America. *Molecules* 23: 544. <https://doi.org/10.3390/molecules23030544>
4. Zohrai HF, Ramazan E, Hariri A (2022) Biological activities and chemical composition of *Rubia tinctorum* (L) root and aerial part extracts thereof. *Acta Biol Colomb* 27: 403–414. <https://doi.org/10.15446/abc.v27n3.95476>
5. Bougateg H, Tandia F, Sila A, et al. (2023) Polysaccharides from baobab (*Adansonia digitata*) fruit pulp: Structural features and biological properties. *S Afr J Bot* 157: 387–397. <https://doi.org/10.1016/j.sajb.2023.04.024>
6. Ebaid H, Bashandy SA, Alhazza IM, et al. (2019) Efficacy of a methanolic extract of *Adansonia digitata* leaf in alleviating hyperglycemia, hyperlipidemia, and oxidative stress of diabetic rats. *BioMed Res Int* 2019: 2835152. <https://doi.org/10.1155/2019/2835152>
7. Abdulrahman MD, Zakariya AM, Hama HA, et al. (2022) Ethnopharmacology, biological evaluation, and chemical composition of *Ziziphus spina-christi* (L.) Desf.: a review. *Adv Pharm Pharm Sci* 2022: 4495688. <https://doi.org/10.1155/2022/4495688>
8. Carvalho LVDN, Cordeiro MF, Sampaio MCPD, et al. (2016) Evaluation of antibacterial, antineoplastic, and immunomodulatory activity of Paullinia cupana seeds crude extract and ethyl-acetate fraction. *Evid-Based Compl Alt* 2016: 1203274. <https://doi.org/10.1155/2016/1203274>
9. Abdulrahman MD, Hamad SW (2022) Traditional methods for treatment and management of measles in Northern Nigeria: medicinal plants and their molecular docking. *Ethnobotany Res Appl* 23. <http://dx.doi.org/10.32859/era.23.33.1-18>
10. Hou T, Wang J (2008) Structure–ADME relationship: still a long way to go? *Expert Opin Drug Met* 4: 759–770. <https://doi.org/10.1517/17425255.4.6.759>
11. An NTG, Huong LT, Satyal P, et al. (2020) Mosquito larvicidal activity, antimicrobial activity, and chemical compositions of essential oils from four species of *Myrtaceae* from central Vietnam. *Plants* 9: 544. <https://doi.org/10.3390/plants9040544>
12. Adeniyi CBA, Lawal TO, Mahady GB (2009) In vitro susceptibility of *Helicobacter pylori* to extracts of *Eucalyptus camaldulensis* and *Eucalyptus torelliana*. *Pharm Biol* 47: 99–102. <https://doi.org/10.1080/13880200802448708>
13. Sabo VA, Knezevic P (2019) Antimicrobial activity of *Eucalyptus camaldulensis* Dehn. plant extracts and essential oils: a review. *Ind Crop Prod* 132: 413–429. <https://doi.org/10.1016/j.indcrop.2019.02.051>
14. Silva J, Abebe W, Sousa S, et al. (2003) Analgesic and anti-inflammatory effects of essential oils of *Eucalyptus*. *J Ethnopharmacol* 89: 277–283. <https://doi.org/10.1016/j.jep.2003.09.007>

15. Abubakar EMM (2010) Antibacterial potential of crude leaf extracts of *Eucalyptus camaldulensis* against some pathogenic bacteria. *Afr J Plant Sci* 4: 202–209. <https://doi.org/10.5897/AJPS.9000020>
16. OO A, Adeniyi BA (2008) The antibacterial activity of leaf extracts of *Eucalyptus camaldulensis* (Myrtaceae). *J Appl Sci Res* 4: 1410–1413. <http://eprints.covenantuniversity.edu.ng/id/eprint/6073>
17. Knezevic P, Aleksic V, Simin N, et al. (2016) Antimicrobial activity of Eucalyptus camaldulensis essential oils and their interactions with conventional antimicrobial agents against multi-drug resistant *Acinetobacter baumannii*. *J Ethnopharmacol* 178: 125–136. <https://doi.org/10.1016/j.jep.2015.12.008>
18. Abdulrahman MD, Hasan Nudin NF, Khandaker MM, et al. (2019) In vitro biological investigations on *Syzygium polyanthum* cultivars. *Int J Agr Biol* 22: 1399–1406. <https://doi.org/10.17957/IJAB/15.1214>
19. Sitthan VK, Abdallah MS, Nallappan M, et al. (2023) Antioxidant and antibacterial activity of different solvent extracts of leaves and stem of *Alyxia reinwardtii* blume. *Malays Appl Biol* 52: 67–80. <https://doi.org/10.55230/mabjournal.v52i6.2581>
20. DOGARA AM (2023) Chemical composition of *Corymbia citriodora*. *Nusant Biosci* 15: 172–178. <https://doi.org/10.13057/nusbiosci/n150205>
21. Mahmoud AD, Ali AM, Khandaker MM, et al. (2019) Discrimination of *Syzygium polyanthum* Cultivars (Wight) Walp based on essential oil composition. *J Agrobiotechnology* 10: 1–9.
22. Yunusa AK, Abdullahi N, Rilwan A, et al. (2018) DPPH Radical scavenging activity and total phenolic content of rambutan (*Nephelium lappaceum*) peel and seed. *Annals: Food Sci Technol* 774–779.
23. Yunusa AK, Rashid ZM, Mat N, et al. (2018) Chemicals and bioactivity discrimination of syconia of seven varieties of *Ficus deltoidea* Jack via ATR-IR spectroscopic-based metabolomics. *Pharmacog J* 10: s141–s151. <http://dx.doi.org/10.5530/pj.2018.6s.27>
24. Nudin NFH, Ali AM, Awang NA, et al. (2019) Discrimination of *Syzygium polyanthum* cultivars (wight) walp based on essential oil composition. *J Agrobiotechnol (Malaysia)* 1–9.
25. Usman M, Abdulrahman MD, Hamad S, et al. (2022) Antioxidants, anti-inflammation, anti-hyperglycemia and chemical evaluation of the whole plant extracts of *Anisopus mannii* N.E. Br. *Zanco J Pure Appl Sci* 34: 114–122. <http://dx.doi.org/10.21271/zjpas>
26. Pettersen EF, Goddard TD, Huang CC, et al. (2004) UCSF Chimera—a visualization system for exploratory research and analysis. *J Comput Chem* 25: 1605–1612. <https://doi.org/10.1002/jcc.20084>
27. Dakpa G, Kumar KJS, Nelen J, et al. (2023) Antcin-B, a phytosterol-like compound from Taiwanofungus camphoratus inhibits SARS-CoV-2 3-chymotrypsin-like protease (3CL^{Pro}) activity in silico and in vitro. *Sci Rep* 13: 17106. <https://doi.org/10.1038/s41598-023-44476-x>
28. Eberhardt J, Santos-Martins D, Tillack AF (2021) AutoDock Vina 1.2. 0: new docking methods, expanded force field, and python bindings. *J Chem Inf Model* 61: 3891–3898. <https://doi.org/10.1021/acs.jcim.1c00203>
29. Kuriata A, Gierut AM, Oleniecki T, et al. (2018) CABS-flex 2.0: a web server for fast simulations of flexibility of protein structures. *Nucleic Acids Res* 46: W338–W343. <https://doi.org/10.1093/nar/gky356>

30. Poojary MM, Vishnumurthy KA, Adhikari AV (2015) Extraction, characterization and biological studies of phytochemicals from *Mammea suriga*. *J Pharm Anal* 5: 182–189. <https://doi.org/10.1016/j.jpha.2015.01.002>
31. Al-Qurainy F, Gaafar A, Khan V, et al. (2013) Antibacterial activity of leaf extract of *Breonadia salicina* (Rubiaceae), an endangered medicinal plant of Saudi Arabia. *Genet Mol Res* 12: 3212–3219. <http://dx.doi.org/10.4238/2013.August.29.5>
32. Danduru AP, Avanti C (2020) Antioxidant activity screening of seven Indonesian herbal extract. *Biodiversitas* 21: 2062–2067. <https://doi.org/10.13057/biodiv/d210532>
33. Noipha K, Suwannarat P, Prom-in S, et al. (2024) Phytochemical, antioxidant and antimicrobial activities of hevea brasiliensis leaves extract. *HAYATI J Biosci* 31: 241–247. <https://doi.org/10.4308/hjb.31.2.241-247>
34. Stagos D (2019) Antioxidant activity of polyphenolic plant extracts. 9: 19. *Antioxidants* <https://doi.org/10.3390/antiox9010019>
35. Ahamad J, Uthirapathy S, Mohammed Ameen MS, et al. (2019) Essential oil composition and antidiabetic, anticancer activity of *Rosmarinus officinalis* L. leaves from Erbil (Iraq). *J Essent Oil Bear Plants* 22: 1544–1553. <https://doi.org/10.1080/0972060X.2019.1689179>
36. Alkefai NH, Ahamad J, Amin S, et al. (2018) Arylated gymnemic acids from *Gymnema sylvestre* R. Br. as potential α -glucosidase inhibitors. *Phytochem Lett* 25: 196–202. <https://doi.org/10.1016/j.phytol.2018.04.021>
37. Abdulrahman MD, Hasan Nudin NF, Khandaker MM, et al. (2019) In vitro biological investigations on *Syzygium polyanthum* cultivars. *Int J Agric Biol* 22: 1399–1406. <https://doi.org/10.17957/IJAB/15.1214>
38. Bharti SK, Krishnan S, Kumar A, et al. (2018) Antidiabetic phytoconstituents and their mode of action on metabolic pathways. *Ther Adv Endocrinol* 9: 81–100. <https://doi.org/10.1177/2042018818755019>
39. Lee JW, Kim NH, Kim JY, et al. (2013) Aromadendrin inhibits lipopolysaccharide-induced nuclear translocation of NF- κ B and phosphorylation of JNK in RAW 264.7 macrophage cells. *Biomol Ther* 21: 216. <https://doi.org/10.4062/biomolther.2013.023>
40. Bakun P, Czarczynska-Goslinska B, Goslinski T, et al. (2021) In vitro and in vivo biological activities of azulene derivatives with potential applications in medicine. *Med Chem Res* 30: 834–846. <https://doi.org/10.1007/s00044-021-02701-0>
41. YELUGUDARI B, MESRAM N, KARNATI PR (2023) 9-Hexadecenoic acid rich HPLC fraction of *Pithecellobium dulce* methanolic seed extract exhibits potential antiinflammatory activity by inhibiting IL-8, IL-6, and PGE2: phytochemical characterization, in-vitro and in-vivo evaluation. *J Res Pharm* 27: 1734. <https://doi.org/10.29228/jrp.458>
42. Khan MS, Uzair M, Hanif M, et al. (2022) Anti-inflammatory potential of spectroscopically analyzed trans-13-octadecenoic acid of *Yucca elephantipes* Regel roots: in-vitro and in-vivo analysis. *Pak J Pharm Sci* 35: 1549. <https://doi.org/10.36721/PJPS.2022.35.6.REG.1549-1556.1>
43. Shityakov S, Förster C (2014) In silico predictive model to determine vector-mediated transport properties for the blood–brain barrier choline transporter. *Adv Appl Bioinform Chem* 7: 23–36. <https://doi.org/10.2147/AABC.S63749>
44. Arthur DE, Uzairu A (2019) Molecular docking studies on the interaction of NCI anticancer analogues with human Phosphatidylinositol 4, 5-bisphosphate 3-kinase catalytic subunit. *J King Saud Univ-Sc* 31: 1151–1166. <https://doi.org/10.1016/j.jksus.2019.01.011>

45. Ortiz CLD, Completo GC, Nacario R, et al. (2019) Potential inhibitors of galactofuranosyltransferase 2 (GfT2): molecular docking, 3D-QSAR, and in silico ADMETox studies. *Sci Rep* 9: 17096. <https://doi.org/10.1038/s41598-019-52764-8>
46. Dibha AF, Wahyuningsih S, Kharisma VD, et al. (2022) Biological activity of kencur (*Kaempferia galanga* L.) against SARS-CoV-2 main protease: In silico study. *Int J Health Sci* 6: 468–480.
47. Chuanphonpanich S, Racha S, Saengsitthisak B, et al. (2023) Computational assessment of Cannflavin A as a TAK1 inhibitor: implication as a potential therapeutic target for anti-inflammation. *Sci Pharm* 91: 36. <https://doi.org/10.3390/scipharm91030036>
48. Umar AK, Zothantluanga JH, Luckanagul JA, et al. (2023) Structure-based computational screening of 470 natural quercetin derivatives for identification of SARS-CoV-2 Mpro inhibitor. *PeerJ* 11: e14915. <https://doi.org/10.7717/peerj.14915>
49. Jacob E , Unger R (2007) A tale of two tails: why are terminal residues of proteins exposed? *Bioinformatics* 23: e225–e230. <https://doi.org/10.1093/bioinformatics/btl318>
50. Mushtaq A, Azam U, Mehreen S, et al. (2023) Synthetic α -glucosidase inhibitors as promising anti-diabetic agents: recent developments and future challenges. *Eur J Med Chem* 249: 115119. <https://doi.org/10.1016/j.ejmech.2023.115119>



AIMS Press

© 2024 the Author(s), licensee AIMS Press. This is an open access article distributed under the terms of the Creative Commons Attribution License (<http://creativecommons.org/licenses/by/4.0>)